arXiv:0905.0352v2 [nucl-th] 1 Feb 2010

Deconfinement Phase Transition in Compact Stars : Maxwell vs. Gibbs Construction of the Mixed Phase

Abhijit Bhattacharyya[1,2], Igor N. Mishustin[2,3] and Walter Greiner[2]
[1] *Department of Physics, University of Calcutta, 92, A. P. C. Road, Kolkata 700 009, India*
[2] *Frankfurt Institute for Advanced Studies, J.W. Goethe–Universität, Ruth-Moufang-Strasse 1, D–60438 Frankfurt am Main, Germany*
[3] *The Kurchatov Institute, Russian Research Center, 123182 Moscow, Russia*

We study different realisations of the first order deconfinement phase transition inside a compact star by comparing the Gibbs and Maxwell construction for the mixed phase. The hadronic sector is described within the relativistic mean field model including hyperons. The quark sector is described by the MIT Bag model. We find that these two realisations lead to very different star properties, in particular, the composition of the stellar matter. We also find that for the Maxwell construction there is a sharp discontinuity in the baryon density and the electron chemical potential. We argue that a sharp jump in the elctron chemical potential should lead to the redistribution of electrons and formation of strong electric fields around the discontinuity surface.

PACS numbers: 14.65.-q, 26.60.+c, 97.10.-q, 98.70.Rz

I. INTRODUCTION

The heavy ion experiments at RHIC, LHC and FAIR are designed to study strongly interacting matter under extreme conditions of high temperature and/or high baryon density. These experiments are also expected to shed light on the properties of a new phase of strongly interacting matter, the Quark Gluon Plasma (QGP) and on the nature of the deconfinement phase transition. On the other hand, compact stars, due to their large central densities, serve as a natural laboratory to study the properties of the strongly interacting matter at high densities and small temperature, in particular, the possibility of a deconfining phase transition.

At finite temperature and zero baryon density, numerical studies on lattice are believed to provide reliable results for the physics of the deconfinement transition [1]. In this case the lattice calculations predict that the deconfinement happens via a smooth crossover transition [2] at a temperature $\sim$ 170 - 200 MeV [3]. However, the studies at finite baryon densities on the lattice are very difficult. Some progress has been made in recent years in extending calculations to finite quark chemical potentials but they do not provide reliable results yet [4, 5]. There is an indication of a critical point at a rather small quark chemical potential $\mu_q \approx 100$ MeV, with a first order transition for larger μ_q [4].

The most recent interest in the study of first order deconfining phase transition is related to the nature of the mixed phase (MP) [6]. Especially, the role of the screened Colulomb potential and interface effects in the MP were studied by several authors (see e.g. refs. [7–11]). A detailed study employing the Wigner Seitz cell approach [7] suggests that the MP behaves more in accordance with that for Maxwell Construction (MC) rather than the Gibbs Construction (GC). Earlier similar questions were addressed in connection with the "pasta" phases associated with the liquid-gas phase transition [12].

In this work we present a comparative study of compact stars with the MC and GC of the mixed phase. For the hadronic phase we use a Relativistic Mean Field (RMF) model of the Walecka type [13]. Besides nucleons, this model contains hyperons as well as hyperon-hyperon interaction. For the quark sector we employ the MIT Bag model [14] which has been used previously for the description of strange quark stars (see a recent review [15]). We construct the MP for the deconfinement phase transition and

obtain the equations of state (EOSs) for the both cases. The next section is devoted to the description of these models and corresponding EOSs. In section 3 we use these EOSs to describe properties of the compact stars. In section 4 we study the jump in the electron chemical potential at the interface between the two phases and estimate an induced electric field. In the last section we summarise our results.

II. PROPERTIES OF MATTER IN COMPACT STARS

A. Hadron phase

At low densities the relevant degrees of freedom are hadrons. To describe the hadronic phase we use a non-linear version of the RMF model. In this model the baryons interact with mean meson fields. The variant that we use here is known as the TM1 model [16].

The Lagrangian density for the TM1 model including both nucleons and hyperons is written as [16, 17]

$$\begin{aligned}\mathcal{L} &= \sum_B \overline{\psi}_B \left(i\partial\!\!\!/ - m_B\right)\psi_B + \frac{1}{2}\partial^\mu\sigma\partial_\mu\sigma - \frac{1}{2}m_\sigma^2\sigma^2 - \frac{b}{3}\sigma^3 - \frac{c}{4}\sigma^4 - \frac{1}{4}\omega^{\mu\nu}\omega_{\mu\nu} + \frac{1}{2}m_\omega^2\omega^\mu\omega_\mu \\ &+ \frac{d}{4}(\omega_\mu\omega^\mu)^2 - \frac{1}{4}\vec{\rho}^{\mu\nu}\vec{\rho}_{\mu\nu} + \frac{1}{2}m_\rho^2\vec{\rho}^\mu\vec{\rho}_\mu + \sum_B \overline{\psi}_B\left(g_{\sigma B}\sigma + g_{\omega B}\omega^\mu\gamma_\mu + g_\rho\vec{\rho}^\mu\gamma_\mu\vec{\tau}_B\right)\psi_B\,, \end{aligned} \tag{1}$$

where the sum runs over all the baryons $B{=}p, n, \Lambda, \Sigma^{0,\pm}, \Xi^{0,-}$. In the above Lagrangian σ, ω and $\vec{\rho}$ are respectively the iso-scalar scalar σ, the iso-scalar vector ω and the isovector vector ρ meson fields. In eq. (1) $\omega^{\mu\nu}$ and $\vec{\rho}^{\mu\nu}$ denote, respectively, the field tensors for the ω and ρ meson fields.

This model is good enough to describe nucleonic matter and the nuclear saturation point. But it is insufficient for the hyperonic matter, because the model does not reproduce the observed strong $\Lambda\Lambda$ attraction. This defect can be remedied by adding two new meson fields with hidden strangeness, namely, the iso-scalar scalar σ^* and the iso-vector vector ϕ, which couple to hyperons only [17]. These fields can be identified with the $f_0(975)$ and $\phi(1020)$ mesons. The corresponding Lagrangian is given by

$$\mathcal{L}^{YY} = \frac{1}{2}\left(\partial^\mu\sigma^*\partial_\mu\sigma^* - m_{\sigma^*}^2\sigma^{*2}\right) - \frac{1}{4}\phi^{\mu\nu}\phi_{\mu\nu} + \frac{1}{2}m_\phi^2\phi^\mu\phi_\mu + \sum_Y \overline{\psi}_Y\left(g_{\sigma^*Y}\sigma^* + g_{\phi Y}\phi^\mu\gamma_\mu\right)\psi_Y$$

where index Y runs over hyperons only.

For a complete description of the beta equilibrated cold matter the model should include leptons; namely electrons and muons. The leptonic part of the lagrangian is

$$\mathcal{L}^l = \sum_{l=e^-,\mu^-} \overline{\psi}_l\left(i\partial\!\!\!/ - m_B\right)\psi_l \tag{2}$$

The Lagrangian density of the complete model, which we call TM1YY, is written as

$$\mathcal{L}^{TM1YY} = \mathcal{L} + \mathcal{L}^{YY} + \mathcal{L}^l \tag{3}$$

The nucleon coupling constants are chosen from the fit of the finite nuclei properties. The vector coupling constants of the hyperons are chosen according to the SU(6) symmetry and the hyperonic scalar coupling constants are chosen to reproduce the measured values of the corresponding optical potentials. Below we use the set of model parameters obtained in ref. [17].

We calculate the energy density and pressure for the TM1YY model in the mean field approximation. They are given by the following expressions

$$\epsilon^H = \frac{1}{2}m_\sigma^2\sigma^2 + \frac{b}{3}\sigma^3 + \frac{c}{4}\sigma^4 + \frac{1}{2}m_{\sigma^*}^2\sigma^{*2} + \frac{1}{2}m_\omega^2\omega_0^2 + \frac{3d}{4}\omega_0^4$$

$$+\frac{1}{2}m_\rho^2\rho_{0,0}^2+\frac{1}{2}m_\phi^2\phi_0^2+\sum_B\frac{\nu_B}{2\pi^2}\int_0^{k_F^B}dk\,k^2\sqrt{k^2+{m_B^*}^2}\,, \tag{4}$$

$$P^H = -\frac{1}{2}m_\sigma^2\sigma^2-\frac{b}{3}\sigma^3-\frac{c}{4}\sigma^4-\frac{1}{2}m_{\sigma^*}^2{\sigma^*}^2+\frac{1}{2}m_\omega^2\omega_0^2+\frac{d}{4}\omega_0^4$$
$$+\frac{1}{2}m_\rho^2\rho_{0,0}^2+\frac{1}{2}m_\phi^2\phi_0^2+\sum_B\frac{\nu_B}{6\pi^2}\int_0^{k_F^B}dk\frac{k^4}{\sqrt{k^2+{m_B^*}^2}}\,, \tag{5}$$

where $m_B^*=m_B-g_{\sigma B}\sigma-g_{\sigma^* B}\sigma^*$ is the effective mass, ν_B is the degeneracy factor and $k_F^B=\sqrt{\mu_B^2-m_B^{*2}}$ is the Fermi momentum of the baryon species B.

B. Quark Phase

At higher densities baryons begin to overlap and loose their individuality. In order to describe the medium the quark degrees of freedom need to be included. The density inside a compact star is high enough to encompass these degrees of freedom. In order to describe the quark phase we adopt the simple MIT Bag model [14], with three flavours (u, d and s). We also add electrons and muons to describe the beta equilibrated matter as in the case of the hadronic phase. For the bag model the energy density and pressure can be written as

$$\epsilon^Q = \sum_{f=u,d,s}\frac{\nu_f}{2\pi^2}\int_0^{k_F^f}dk k^2\sqrt{m_f^2+k^2}+B\,, \tag{6}$$

$$P^Q = \sum_{f=u,d,s}\frac{\nu_f}{6\pi^2}\int_0^{k_F^f}dk\frac{k^4}{\sqrt{m_f^2+k^2}}-B\,, \tag{7}$$

where $k_F^f=\sqrt{\mu_f^2-m_f^2}$ is the Fermi momentum of quarks with flavor f. For each flavor we choose the degeneracy factor $\nu_f=2\,(\text{spin})\times 3\,(\text{color})=6$ and take the following values of quark masses: $m_u=5$ MeV, $m_d=10$ MeV and $m_s=150$ MeV.

It is worth noting that because of the negative vacuum pressure ($-B$ in eq.(7)) the Bag model EOS always has a zero pressure at a finite baryon density, $\rho_B^*\sim B^{3/4}$. By this reason the equilibrium configurations of the strange quark matter (SQM) may exist even without gravity [18]. They should have a sharp boundary with the density jump from ρ_B^* to zero. The EOS derived from the NJL model has the similar property [19].

C. Construction of the mixed phase and EOS

We are studying the electrically neutral stellar matter in beta equilibrium. Under such conditions the chemical potential of a particle species i can be written as

$$\mu_i = B_i\,\mu_B+Q_i\,\mu_Q \tag{8}$$

where B_i is the baryon number of the species i , Q_i denotes its charge in units of the electron charge, μ_B and μ_Q are the baryonic and electric chemical potentials, respectively. Here we assume that neutrinos can freely escape from the star. The above equation signifies that only those reactions are allowed which conserve charge and baryon number, however strangeness is not conserved. Two independent chemical potentials, μ_B and μ_Q, are found by fixing the baryon and electric charge densities:

$$\rho_B=\sum_i B_i\rho_i\,,\qquad \rho_Q=\sum_i Q_i\rho_i\,, \tag{9}$$

where ρ_i is the number density of the particle species i. We require electrical neutrality of a star on a macroscopic scale, *i.e.* $\bar{\rho}_Q = 0$. According to Eq. (8), the baryon chemical potential μ_B equals the neutron chemical potential μ_n and μ_Q is equal to the electron chemical potential μ_e. At given μ_B and μ_Q, the quark chemical potentials are found by using the formulae $\mu_u = (\mu_B - 2\,\mu_Q)/3$ and $\mu_d = \mu_s = (\mu_B + \mu_Q)/3$.

As indicated by the model calculations (see e.g. ref.[20]) the deconfinement phase transition, at high densities, is of first order in nature. So this transition should produce a MP between a pure hadronic and a pure quark phase. There are two ways by which one can construct the MP: the Maxwell construction (MC) and the Gibbs construction (GC). Below we consider both possibilities.

The Gibbs conditions for the mixed phase are

$$P_1(\mu_B, \mu_Q) \;=\; P_2(\mu_B, \mu_Q)\,, \tag{10}$$

$$\mu_B \;=\; \mu_{B1} \;=\; \mu_{B2}\,, \tag{11}$$

$$\mu_Q \;=\; \mu_{Q1} \;=\; \mu_{Q2}\,. \tag{12}$$

Here and below 1 stands for the hadronic phase and 2 stands for the quark phase.

It is well known that in the case of two chemical potentials the Gibbs conditions (10) - (12) can be fulfilled only if the coexisting phases have opposite electric charges and the condition of global neutrality is imposed [21]. This condition can be written as

$$\bar{\rho}_Q = (1-\lambda)\,\rho_{Q1}(\mu_B, \mu_Q) + \lambda\,\rho_{Q2}(\mu_B, \mu_Q) = 0\,. \tag{13}$$

Then the volume averaged energy density in the MP is calculated as

$$\bar{\epsilon} \;=\; (1-\lambda)\,\epsilon_1(\mu_B, \mu_Q) + \lambda\,\epsilon_2(\mu_B, \mu_Q)\,, \tag{14}$$

where $\lambda = V_2/V$ is the volume fraction of quark phase.

Thus, the mixed phase is a very inhomogeneous state of matter with intermittent domains of two different phases. Therefore realistic approaches must take into account not only differences in the bulk properties of these phases, but also additional contributions to the thermodynamic potential coming from the interface energy and electrostatic energy associated with theses domains. First attempt to perform such calculations have been done in [22] but due to significant uncertainties in the model parameters, as *e.g.* interface energy, the results are not conclusive yet. As pointed out in ref. [7], it may happen that the GC mixed phase is energetically too expensive and may be expelled from the star at all. Then the situation is closer to the MC case, where two pure phases are in direct contact with each other. This situation corresponds to the Maxwell construction of the mixed phase defined by the conditions :

$$P_1(\mu_B, \mu_Q) \;=\; P_2(\mu_B, \mu_Q) \tag{15}$$

$$\mu_B \;=\; \mu_{B1} \;=\; \mu_{B2} \tag{16}$$

They mean that the baryon chemical potential is continuous, but the electric chemical potential μ_Q jumps at the interface between the two phases. Also, contrary to the Gibbs construction, where the pressure in the mixed phase increases with baryon density, Maxwell construction corresponds to constant pressure in the density interval of the mixed phase.

Figures 1a and 1b show the equations of state obtained with GC and MC for two cases, $B^{1/4} =$ 180 MeV and 185 MeV, respectively. As can be seen from Fig. 1a, for MC the mixed phase starts at $\rho_B = 0.41\,\mathrm{fm}^{-3}$ and ends at $0.68\,\mathrm{fm}^{-3}$, whereas for the GC these values are $0.23\,\mathrm{fm}^{-3}$ and $0.89\,\mathrm{fm}^{-3}$ respectively. So in the case of GC the phase transition starts early and the width of the MP region is much boader compared to that in MC. As one increases the Bag constant B the width of the MP region further increases for GC, as can be seen in Fig. 1b. In this case the MP starts at $\rho_B = 0.26\,\mathrm{fm}^{-3}$ and

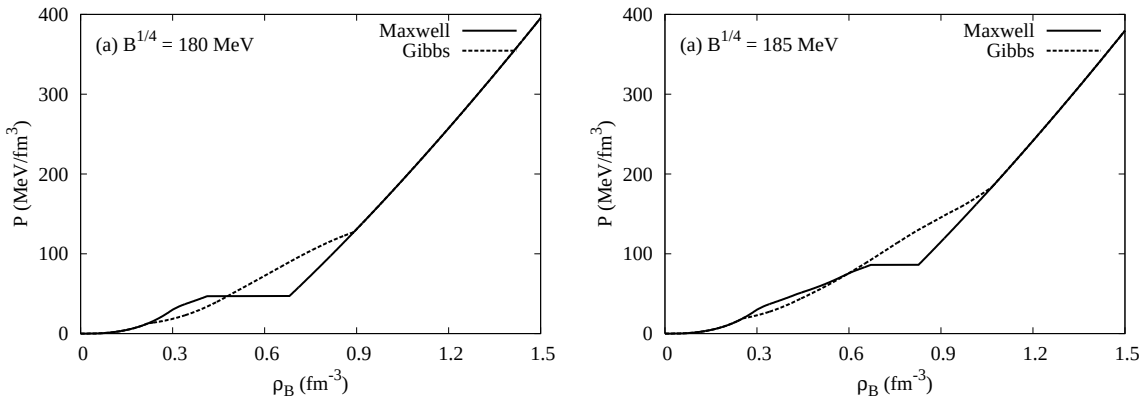

FIG. 1: Equations of state for a) $B^{1/4} = 180$ MeV and b) $B^{1/4}$ =185 MeV, for Maxwell and Gibbs construction of the mixed phase.

ends at $1.06\,\mathrm{fm}^{-3}$. On the other hand, for the MC the width of the MP region decreases. For this case the MP starts at $\rho_B = 0.67\,\mathrm{fm}^{-3}$ and ends at $0.83\,\mathrm{fm}^{-3}$. These results will certainly affect the star properties which we will discuss in the next section.

In Fig. 2 we have plotted the particle abundances for all the cases discussed above. In Figs. 2a and 2b the results are for $B^{1/4} = 180$ MeV, for the MC and GC, respectively. From Fig. 2b, *i.e.* for GC, we see that only one hyperon, *i.e.* Λ, is present in the medium. On the other hand, for the case of MC (Fig. 2a) both Σ^- and Λ hyperons appear in the medium. This happens because in the case of GC the phase transition starts early, and as a result, hyperons can appear only in the MP. However due to the presence of the strange quark, hyperon production in the MP is suppressed and as a result Σ^- does not appear at all. For MC the phase transition starts much later allowing the Σ^- to appear in the hadronic phase. It is interesting that the case of $B^{1/4} = 185$ MeV exhibits a completely different picture as shown in Figs. 2c and 2d. Firstly, in the case of GC, the MP region is broader as compared with the case of $B^{1/4} = 180$ MeV. This allows almost all the hyperons, except Ξ^0, to be present in the matter, the Σ^- appears after Λ. For the case of MC, as the MP begins at a higher density, almost all the hyperons are present in the hadronic phase. But, contrary to the case of GC, the Σ^- appears before Λ. So the particle cocktail is rather different for the two constructions.

III. PROPERTIES OF COMPACT STARS

Having obtained the EOSs and the particle abundances we now calculate the properties of compact stars with the deconfinement phase transition. We treat the matter to be an ideal fluid and obtain the star structure by solving the TOV equations with the corresponding EOS as an input (see details in [23]). The masses and radii of stars are calculated as a function of the central baryon density. Results of our calculations for MC and GC are shown in Figs. 3a and 3b, for $B^{1/4} = 180$ MeV and 185 MeV, respectively.

In Fig. 3a one can see that the maximum mass for the MC is noticeably higher than that for the GC case. The values are $1.493 M_\odot$ and $1.396 M_\odot$ respectively. This happens because in the MC the phase transition starts quite late compared to the GC, that allows the star to stay longer in the hadronic phase. Moreover, for the MC case there is a range of central baryon densities, from $0.41\,\mathrm{fm}^{-3}$ to $0.68\,\mathrm{fm}^{-3}$, corresponding to the MP, which are not allowed in the star. As a result there appears a plateau over

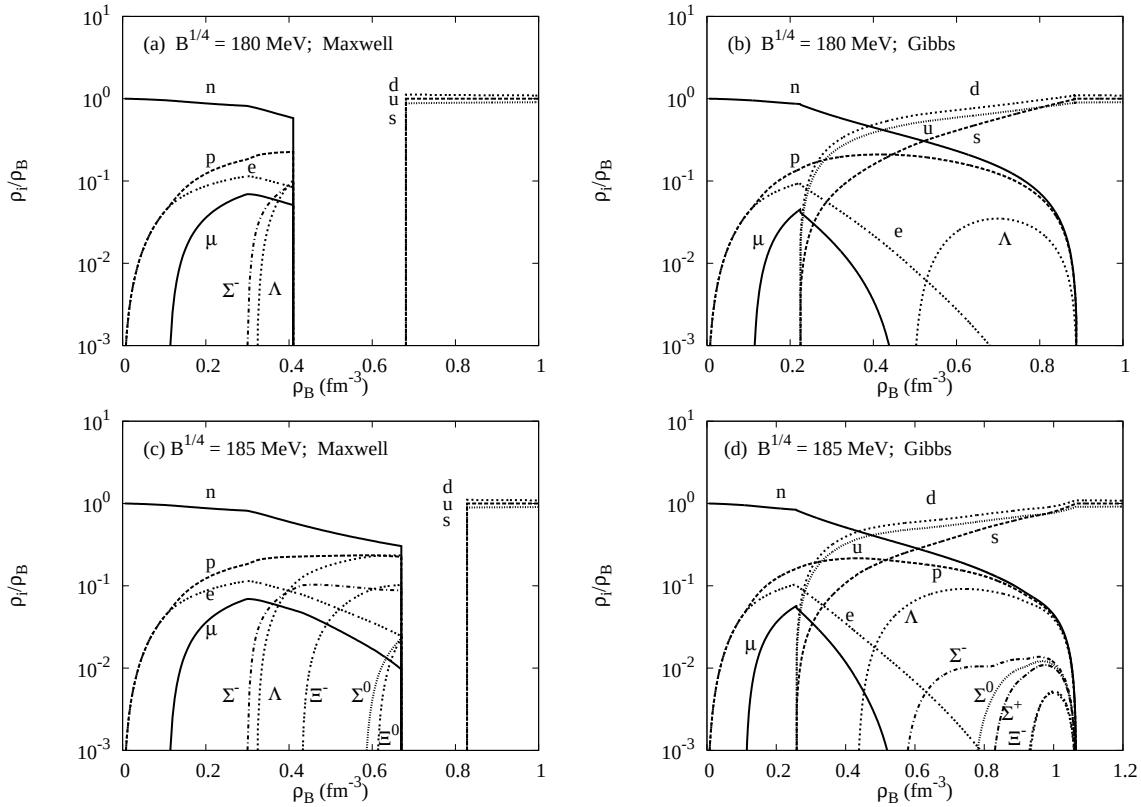

FIG. 2: Particle compositions for a) $B^{1/4} = 180$ MeV MC, b) $B^{1/4} = 180$ MeV GC, c) $B^{1/4} = 185$ MeV MC and d) $B^{1/4} = 185$ MeV GC.

this range of central baryon densities. As calculations show, stable star configurations are located on the left side of the plateau *i.e.* till the point A. The region from A to B is not accessible inside the star. On the right side of the plateau there is a region, from B to C, where the mass decreases with increasing central baryon density, that corresponds to be the unstable configurations. Another interesting feature of the MC stars is the appearance of the growing portion of the curve between C and D. This gives rise to a new family of stable stars (twin stars) around the mass of $1.34M_\odot$ similar to the situation studied in ref. [20]. However there is no such a stable solution for GC. The main difference of twin stars from the normal neutron stars is that they contain a large quark matter core (see also Fig. 5a).

For $B^{1/4} = 185$ MeV the maximum masses are $1.567M_\odot$ and $1.466M_\odot$ for the MC and GC cases respectively. The forbidden range of baryon densities for the MC case is much smaller, ranging from $0.67\,\mathrm{fm}^{-3}$ to $0.83\,\mathrm{fm}^{-3}$ only. However, there is no stable twin star solution for this value of the Bag pressure. This situation can be explained from the well known fact that a significant quark core can appear only if the density jump is large enough [24].

The features discussed above are even more obvious if one looks at the mass-radius plots shown in Fig. 4. As one can see in Figs. 4a and 4b the mass-radius relations are very different for MC and GC stars. Furthermore, the appearance of two maxima associated with the twin stars is very obvious in Fig. 4a. The cusps in the MC curves correspond to the plateau regions of Figs. 3a,b.

We have calculated also the baryon density profiles of MC and GC stars for the same central density. They are given in Figs. 5a and 5b. Figure 5a shows a sudden jump in the baryon density for the MC case whereas in the GC case the profile is smooth. As Fig. 5b shows there is no jump for the case $B^{1/4}$

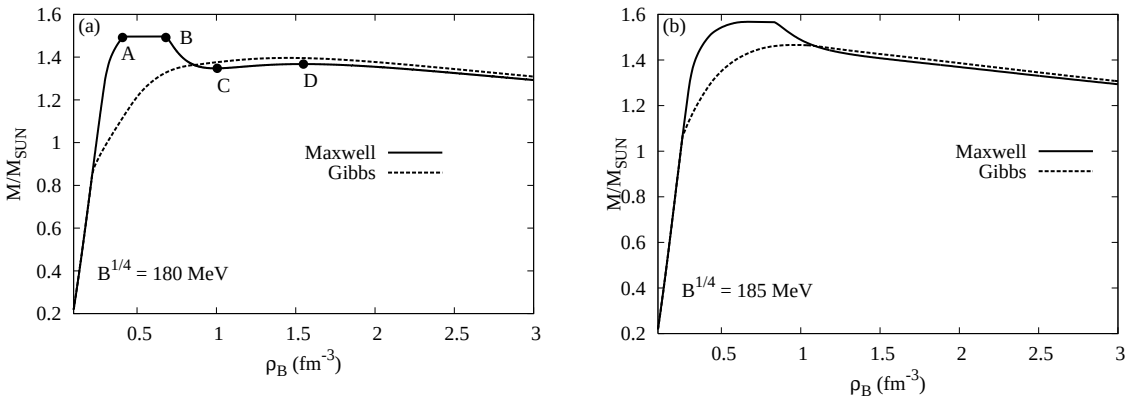

FIG. 3: Mass of a star (in solar units) as a function of baryon density for a) $B^{1/4} = 180$ MeV and b) $B^{1/4}$ =185 MeV. See text for further explanation.

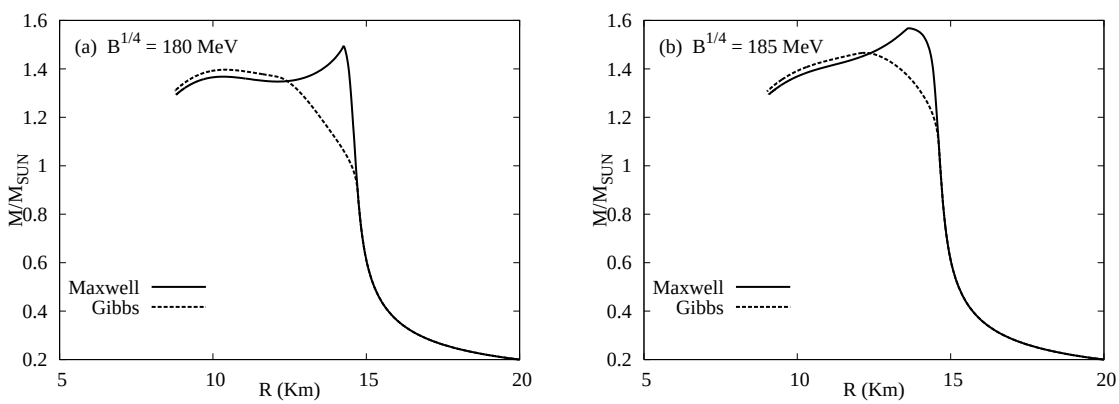

FIG. 4: Mass-Radius relation of the stars for a) $B^{1/4} = 180$ MeV and b) $B^{1/4} = 185$ MeV.

= 185 MeV and there is no stable star with a quark core.

IV. JUMP IN ELECTRON CHEMICAL POTENTIAL

In this section we discuss possible implications of the jump in the baryon density of the MC stars as illustrated in Fig. 5a. Figure 6 shows the radial profiles of the electron chemical potential μ_e for the case of $B^{1/4} = 180$ MeV. As expected, in the GC case μ_e evolves smoothly over the mixed phase reaching almost zero in the pure quark phase. But in the MC case μ_e has a jump at the transition between hadronic and quark phases. In the quark core μ_e is very low about 10 MeV and is almost constant, but in the hadronic phase μ_e jumps to a high value, about 196 MeV. Then at larger radii μ_e evolves slowly and finally decrease to small values as one approaches the crust.

This is an interesting situation in the sense that such a discontinuity in the chemical potential of electrons would lead to the flow of electrons across the discontinuity surface from the region with higher μ_e to the region with lower μ_e inside the star. This flow will be terminated by the electric field generated

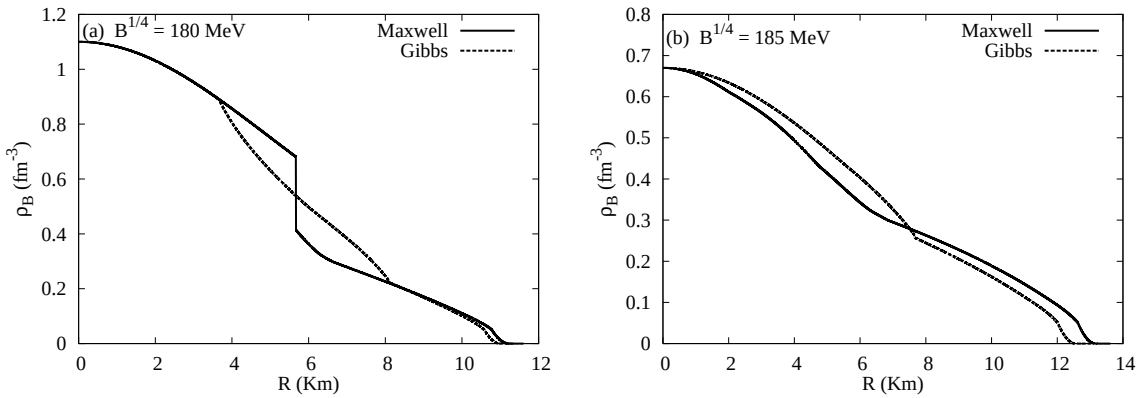

FIG. 5: Comparison of baryon density profiles for MC and GC stars calculated for a) $B^{1/4} = 180$ MeV and b) $B^{1/4} = 185$ MeV.

due to the charge separation. The equilibrium condition can be expressed as

$$\mu_{e1} - e\Phi_1 = \mu_{e2} - e\Phi_2 \tag{17}$$

where μ_{e1} and μ_{e2} are the electron chemical potentials in the hadronic and quark phases, and $\Phi_{1,2}$ are the electrostatic potentials far away from the discontinuity.

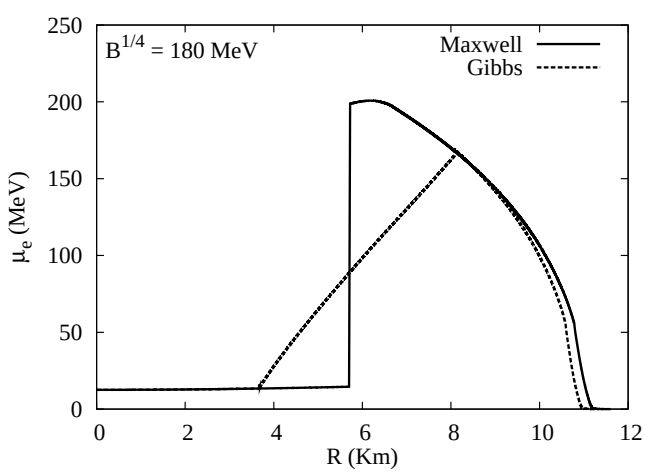

FIG. 6: Profiles of electron chemical potential for MC and GC stars for $B^{1/4} = 180$ MeV.

The profile of the electrostatic potential $\Phi(r)$ over the discontinuity surface can be found from the Poisson equation in combination with the Thomas-Fermi approximation for the electron density $\rho_e(r) = \frac{k_F^3(r)}{3\pi^2}$ where $k_F(r)$ is the local Fermi momentum of the electrons (see details in ref.[25]). In the ultrarelativistic limit $\mu_1 >> m_e$, $\mu_2 >> m_e$, the result can be obtained in the analytic form and the maximum electric field is expressed as

$$E_0 = \frac{\mu_{e1}\mu_{e2}}{e\pi} \times \frac{\mu_{e1} - \mu_{e2}}{\mu_{e1} + \mu_{e2}} \tag{18}$$

For the particular case shown in Fig. 6 we have $\mu_{e1} = 10$ MeV and $\mu_{e2} = 196$ MeV, that gives $E_0 \approx 3$ MV/fm. This is a very strong field, about 1000 times the critical field needed for the spontaneous

electron-positron pair production in vacuum. In fact, this pair production process is Pauli blocked in the considered case. Nevertheless, such a strong electric field may lead to interesting phenomena such as e.g. generation of strong magnetic field in the rotating stars. The generation of strong electric fields at the bare boundary of a quark star was first discussed in ref. [26].

V. SUMMARY

To summarise, we have compared the Gibbs and Maxwell constructions of the mixed phase in the context of deconfinement phase transition in compact stars. For this purpose we have used a RMF model (TM1YY) for the hadronic phase and the MIT Bag model for the quark phase. We have found that the EOSs are very different in these two cases: the MP region occupies a much broader density interval for GC as compared with the MC one. As we increase the Bag constant the width of the MP region in case of GC increases whereas it reduces for the MC case. The particle compositions are also found to be very different for the two cases. We then use these EOSs to calculate the star characteristics. The maximum mass is found to be different for the MC and GC cases. Furthermore, for $B^{1/4}$=180 MeV a stable solution corresponding to second family of compact stars is obtained for MC. The baryon density profiles show a sharp jump for the MC case.

We have also studied the behaviour of the electron chemical potential μ_e across the star and found that it jumps sharply, for MC, at the phase transition boundary. The jump is about 185 MeV for $B^{1/4} =$ 180 MeV. We point out that this jump will lead to redistribution of electrons and generation of a strong electric field at the phase transition boundary. We are planning to study this interesting effect in the future.

Acknowledgements

The authors thank L. M. Satarov for fruitful discussions. The work of AB was partially supported by Alexander von Humboldt Foundation, Council of Scientific and Industrial Research (India) and UGC (UPE & DRS grant). AB also thanks FIAS for the kind hospitality. This work was partly supported by the DFG grant 436 RUS113/711/0-2 and the grants RFFI 09-02-91331, NS-3004.2008.2 (Russia).

[1] F. Karsch, J. Phys. **G35**, 104096 (2008).
[2] Y. Aoki, G. Endrodi, Z. Fodor, S. D. Katz and K. K. Szabo, Nature **443**, 675 (2006).
[3] M. Cheng *et.al.*, Phys. Rev. D **74**, 054507 (2006); Z. Fodor, K. Holland, J. Kuti, D. Nogradi and C. Schroeder, JHEP 0908:084 (2009); Y. Aoki, Z. Fodor, S. D. Katz and K. K. Szabo, Phys. Lett. B **643** 46 (2006).
[4] Z. Fodor and S.D. Katz, JHEP **0404**, 050 (2004); C.R. Allton *et. el.*, Phys. Rev. D **68**, 014507 (2003); R. Gavai and S. Gupta, Phys. Rev. D **78**, 114503 (2008).
[5] P. de Forcrand and O. Philipsen, Nucl. Phys. B **673**, 170 (2003).
[6] N. K. Glendenning, Phys. Rept. **342**, 393 (2001); A. W. Steiner, M. Prakash and J. M. Lattimer, Phys. Lett. B **486**, 239 (2000); M. Alford, K. Rajagopal, S. Reddy and F. Wilczek, Phys. Rev. D **64**, 074017 (2001).
[7] T. Maruyama, T. Tatsumi, T. Endo and S. Chiba, Recent Res. Devel. Phys. **7**, 1 (2006).
[8] T. Maruyama, T. Tatsumi, D. N. Voskresensky, T. Tanigawa and S. Chiba, Nucl. Phys. A **749**, 186 (2005).
[9] T. Maruyama, S. Chiba, H. Schulze and T. Tatsumi, Phys. Lett. B **659**, 192 (2008).
[10] D. N. Voskresensky, M. Yasuhira and T. Tatsumi, Phys. Lett. B **541**, 93 (2002).
[11] T. Maruyama, S. Chiba, H. Schulze and T. Tatsumi, arXiv:0901.2622 [nucl-th].

[12] D. G. Ravenhall, C. J. Pethick and J. R. Wilson, Phys. Rev. Lett. **50**, 2066 (1983); C. J. Horowitz, Eur. Phys. J. A **30**, 303 (2006).
[13] B. D. Serot and J. D. Walecka, Adv. Nucl. Phys. **16**, 1 (1986).
[14] A. Chodos, R. L. Jaffe, K. Johnson, C. B. Thorn, and V. F. Weisskopf, Phys.Rev. D **9**, 3471 (1974).
[15] I. Bombaci, arXiv:0809.4228[gr-qc].
[16] Y. Sugahara and H. Toki, Nucl. Phys. **A579**, 557 (1994).
[17] J. Schaffner and I. Mishustin, Phys. Rev. C **43**, 1416 (1996).
[18] E. Farhi and R. L. Jaffe, Phys. Rev. D **30**, 2379 (1984).
[19] M. Hanauske, L. M. Satarov, I. N. Mishustin, H. Stöcker, and W. Greiner, Phys. Rev. D **64**, 043005 (2001).
[20] I. N. Mishustin, M. Hanauske, A. Bhattacharyya, L. M. Satarov, H. Stöcker, and W. Greiner, Phys. Lett. **B552**, 1 (2003).
[21] N. K. Glendenning, Phys. Rev. D **46**, 1274 (1992).
[22] H. Heiselberg, C. J. Pethick and E. F. Staubo Phys. Rev. Lett. **70**, 1355 (1993).
[23] N. K. Glendenning, *Compact Stars* (Springer, New York, 1997).
[24] A. B. Migdal, A. I. Chernoutsan, and I. N. Mishustin, Phys. Lett. **B83**, 158 (1979); P. Haensel, J. L. Zdunik and R. Schaeffer, Astron. Astrophys. **160**, 121 (1986).
[25] I. Mishustin, C. Ebel, W. Greiner and R. Ruffini, *To be published*.
[26] C. Alcock, E. Farhi and A. Olinto, Astrophys.J. **310**, 261, (1986).